Potential of single-family houses to reinforce resilience in a large scale power system during severe power deficit conditions

Energy Conversion and Management: X 29 (2026) 101570

Contents lists available at ScienceDirect

Energy Conversion and Management: X

journal homepage: www.sciencedirect.com/journal/energy-conversion-and-management-x

Potential of single-family houses to reinforce resilience in a large scale power system during severe power deficit conditions

Sindhu Kanya Nalini Ramakrishna *, Torbjörn Thiringer, Peiyuan Chen

Division of Electric Power Engineering, Chalmers University of Technology, Sweden

ARTICLE INFO

Keywords:
Heat pump
Flexibility
Space heating
Water heating
Single-family houses
Modified Nordic-32 bus system

ABSTRACT

To estimate the potential to reinforce resilience in a power system under severe power deficit conditions, this study investigates the flexibility of space and water heating systems equipped with heat pumps in approximately one million single-family houses. The main contribution lies in the quantification of available power and corresponding duration of reduced power linked to the thermal comfort consequence of these resilience efforts. In this context, an integrated physics-based model is developed that involves a heat pump with space and water heating systems. For the power system with a dimensioning fault of 1.45 GW, the flexibility levels found range between 2.1 GW and 0.5 GW, at outdoor temperatures ranging between −10 °C and 10 °C respectively. An example result is that the power system can be relieved with 2.1 GW for 5 h and 0.8 GW for the next 12 h, with a consequence of the indoor and water temperatures dropping from 20 °C and 55 °C, to 15 °C and 44 °C, respectively at −10 °C outdoor temperature. Furthermore, the average electric power consumption increases to 2.9 GW during the recovery of indoor temperatures over 24 h. Finally, a modified Nordic-32 bus system with a large share of renewable power installations is proposed. In this system, the role of flexibility is demonstrated in limiting the instantaneous frequency deviation during the loss of a major generation. Thus, this study clearly shows the potential of single-family houses to reinforce resilience for a duration ranging from seconds to several hours.

1. Introduction

A future renewable power system is expected to have a production mix that mainly comprises hydro, wind, and solar power installations. To meet the ever-growing electricity demand, the share of wind and solar power installations is expected to increase. Thus, the percentage of plannable power is lower, especially during windy or sunny weather conditions. Furthermore, the amount of plannable power from hydro-electric plants in areas with geographical possibilities could be limited by operational constraints [1]. For example, a dry season followed by long periods of cold weather could lead to periods of low levels of hydro reservoirs. The possibilities of importing power from surrounding regions might be limited due to similar prevailing weather conditions or the loss of major transmission lines, for a duration in the range of several hours. During such a scenario, the lack of preparedness for a major power crisis can lead to blackouts, for example, the Texas power outage in 2021 [2]. An alternative way to strengthen resilience during such severe power deficit conditions is to use the existing heat pump pool as a flexible resource.

Taking Sweden as an example, the total consumption of electric energy is highest in single-family homes in the residential sector [3,4]. Furthermore, about half of the electric energy in these houses is used for space and water heating [5]. In most single-family houses, hydronic heat pumps are used to provide space and water heating, since water-based heating with radiators is the most common solution. Typically, there is no storage tank for space heating. In addition, increasing emphasis on energy efficiency measures will result in the replacement of fixed-speed heat pumps (FSHP) by inverter-driven variable-speed heat pumps (VSHP). In this context, the main aim of this article is to quantify the flexibility of space and water heating systems in single-family houses, equipped with VSHPs.

The performance of a heat pump is indicated by the coefficient of performance (COP). It is the ratio of heat delivered to the amount of electricity consumed. COP is a key parameter in the literature for estimating electricity consumption [6].

There are a number of valuable scientific contributions on using heat pumps as a flexible load. For instance, [7,8] deals with the quantification of the flexibility of heat pumps. Refs. [9,10] involve the investigation of heat pumps as flexible resources. In these articles, explicit mathematical models of COP or the heat pump are missing to estimate electricity consumption under various operating conditions.

* Corresponding author.
E-mail address: kanya@chalmers.se (S.K. Nalini Ramakrishna).

https://doi.org/10.1016/j.ecmx.2026.101570
Received 22 July 2025; Received in revised form 26 September 2025; Accepted 13 January 2026
Available online 15 January 2026

Nomenclature

h_x	Enthalpy in a given state x.
$\dot{m}$	Mass flow rate of the refrigerant that undergoes subcooling in the economiser.
$\dot{m}_{inj}$	Mass flow rate of the injected refrigerant vapour.
P_{comp}	Electric power consumed by the heat pump compressor.
Q_{heat}	Actual value of the heat delivered considering the limitations in the radiators and the heat pump.
Q_{heat}^{*}	Reference value of the heat considering limitations in heat emitters.
Q_{heat}^{**}	Reference value of the desired heat.
T_{cond}^{*}	Estimated condenser temperature of the heat pump.
T_{return}	Water return temperature.
T_{room}	Room temperature.
T_{room}^{*}	Room temperature reference.
T_{source}	Source temperature of the heat pump.
T_{supply}	Water supply temperature.
T_{water}	Water temperature in the domestic hot water tank.
T_{water}^{*}	Water temperature reference.
$T_{water,average}$	Average water temperature in the location where the hot water coil is placed inside the domestic hot water tank.
$\hat{T}_{return}$ *	Estimated value of the return temperature in the heat emitters.
$\hat{T}_{supply}$ *	Estimated value of the desired supply temperature in the heat emitters.
U_{value}	Heat transfer coefficient of the house.
η_{isent}	Isentropic efficiency.

Articles [11–14] deal with frequency support from heat pumps. In [12,14], the operation of the on–off heat pump is considered and the electric power consumption of the heat pumps is constant. Furthermore, in articles [11,13], COP is assumed to be a constant value. Consequently, the flexibility potential cannot be adequately estimated as the COP changes under different operating conditions.

There are valuable articles on the use of heat pumps for demand-side management and primary frequency support. For example, articles [15–19] involve demand-side management using heat pumps. Ref. [20] deals with the flexibility assessment of a residential heat pump pool and [21] with the primary frequency support of heat pumps. In articles [15–21], the empirical formulas used for the estimation of COP differ from one article to another, indicating the limitation to specific heat pumps when using empirical modelling.

Article [22] deals with the enhancement of energy flexibility in residential buildings using VSHPs. These heat pumps are typical ones used in single-family houses. Ref. [23] uses a heat pump as a resource for demand response. In these articles, black boxes are used to estimate COP and electricity consumption, respectively.

Refs. [24,25] deal with grid frequency regulation through a VSHP. Here, COP models are data-driven.

The cost savings utilising thermal flexibility in residential buildings equipped with VSHPs is shown in [26]. Ref. [27] analyses the demand response potential of heat pumps in the German energy system. In these articles, the COP is obtained from the data sheet of the respective heat pumps under specific conditions only.

Articles [22–27] are unfortunately system-specific and it is challenging to adapt the model for different types of heat pumps.

In summary, lacking in the scientific literature [7–27], has been an effort to construct a reproducible and adaptable physics-based model of a heat pump considering operational limitations, to estimate electricity consumption under various conditions. Furthermore, data-driven or black-box models used are data-intensive and quite challenging to adapt if the conditions vary. Thus, the models presented in [7–27] are system-specific and cannot be used for any heat pump by changing the desired parameters as in the case of a physics-based model.

Today, the operation of heat pumps at low source temperatures and the heat delivery capability are improved using vapour injection technology [28]. Neglecting these aspects can result in inaccuracies in flexibility quantification. Furthermore, the heat pumps dealt with in the above literature, excluding [22], do not represent the typical heat pump setup used in single-family houses. In addition, most of the above articles lack a physics-based model of a domestic hot water tank with stratification, heated by circulating hot water through a coil placed inside the tank — with some exceptions, such as Ref. [18]. Methods for estimating water supply temperatures for space and water heating are largely missing. Article [20] is an exception, which presents empirical models for only space heating. However, the corresponding information on indoor temperature is missing. Finally, all of the above studies focus on supporting the power system during normal conditions and not during emergency periods that lead to severe power deficit conditions.

The following are the limitations identified based on the review of previous work carried out.

- The literature lacks a reproducible and adaptable physics-based model of a variable-speed heat pump to estimate electric power consumption under various operating conditions. Furthermore, the operation of heat pumps at low source temperatures using vapour injection technology is often overlooked in the literature.
- Most studies do not reflect the typical setup in Swedish single-family houses, where a heat pump is used for both space and water heating without a storage tank for space heating.
- Methods for estimating water supply temperatures for space and water heating are largely missing.
- Existing studies rarely include physics-based models of domestic hot water tanks, including thermal stratification, where heating is carried out by circulating hot water through a coil inside the tank.

With this background, the main contributions of this paper are as follows.

- A reproducible and adaptable physics-based model of a variable-speed heat pump with vapour injection is developed.
- A physics-based model of a space and water heating system with a heat pump is presented. The system has no storage tank for space heating and has priority set for water heating.
- Controllers for space and water heating systems that involve dynamic estimation of the water supply temperatures are proposed to meet different heating requirements under various operating conditions.
- A physics-based model of a domestic hot water tank with thermal stratification is developed, where the heating is performed by passing hot water through the coil placed in the tank.

The additional contributions apart from addressing the limitations are as follows.

- For outdoor ambient temperatures ranging from −10 °C to 10 °C, flexibility is quantified in terms of instantaneous power reduction and the corresponding duration with respect to normal conditions. The reduction in electric energy during the flexibility period and the net reduction in electric energy considering the recovery period with respect to the normal condition is also quantified.
  - For space heating, in addition to the use of the heat transfer coefficient and the thermal mass of the house, heat losses due to infiltration and natural ventilation are included. The heat recovery of the heat loss from ventilation is also taken into account.

– Inclusion of single-family houses with different thermal properties, equipped with different types of heat pumps, to obtain a comprehensive understanding of the electric power consumption of heating systems.

- Quantification of performance comparison between a FSHP and an VSHP. In addition, the performance difference of a physics-based model of a VSHP is quantified with empirical models.
- Quantification of the importance of planning for a recovery period, in order to not cause 'follow-up problems'.
- A modified Nordic-32 bus system is proposed with a large share of renewable power installations. In this system, the role of flexibility is demonstrated in limiting the instantaneous frequency deviation during the loss of a major generation.

2. Methods

2.1. Representation of heating system in single-family houses equipped with a heat pump

A heat pump providing both space and water heating is shown in Fig. 1. The heat delivered is used to heat water, which in turn is used for either space or water heating, with a priority set for the latter. If the heat delivered is insufficient to provide space heating, additional heating will be provided by the electric heater present before the three-way valve. However, for water heating, the electric heater inside the water tank sometimes provides additional heating.

2.2. Physics based heat pump modelling and operation

Enhanced Vapour Injection (EVI) technology in heat pumps has gained attention in recent years, with the objective of improving the performance, especially in cold climates. Thus, it is important to consider this new feature in studies related to electricity consumption.

The operating region (safe operating conditions) and the COP of a heat pump are increased by incorporating vapour injection in the heat pump cycle. This technology is known as EVI. The representation of vapour injection in a heat pump and in a pressure enthalpy diagram is shown in Figs. 1 and 2, respectively.

Here, the vapour is injected at an intermediate temperature between the evaporator and the condenser temperatures. A part of the liquefied refrigerant with an amount '$\dot{m}$' after subcooling in the condenser flows into a heat exchanger. The other part of the refrigerant with an amount '$\dot{m}_{inj}$' initially flows through an expansion valve and then enters the heat exchanger of the economiser as shown in Fig. 1. In the heat exchanger of the economiser, the heat released by '$\dot{m}$' during subcooling is absorbed by '$\dot{m}_{inj}$'. Subsequently, as '$\dot{m}_{inj}$' is superheated, it is injected into the compressor through an injection port. Thus, the compressor will compress the vapour twice. The first compression is the compression of the superheated vapour at the outlet of the evaporator. The second compression is the compression of the sum of superheated injected vapour and the vapour compressed from the first compression. The various states of a refrigerant are shown both in Fig. 1 and in Fig. 2 within the brackets.

The detailed procedure for estimating the COP of a heat pump with vapour injection is presented in [30]. The key aspects in modelling a heat pump with vapour injection are briefly dealt with below:

- The mass flow rate of the injected vapour '$\dot{m}_{inj}$' is calculated based on the energy balance equation in the economiser and is given by

$$\dot{m}_{inj} = \frac{\dot{m}(h_{3-2} - h_{3-1})}{(h_5 - h_{3-2})} \tag{1}$$

Here, 'h' represents the specific enthalpy in a state indicated in the subscript.

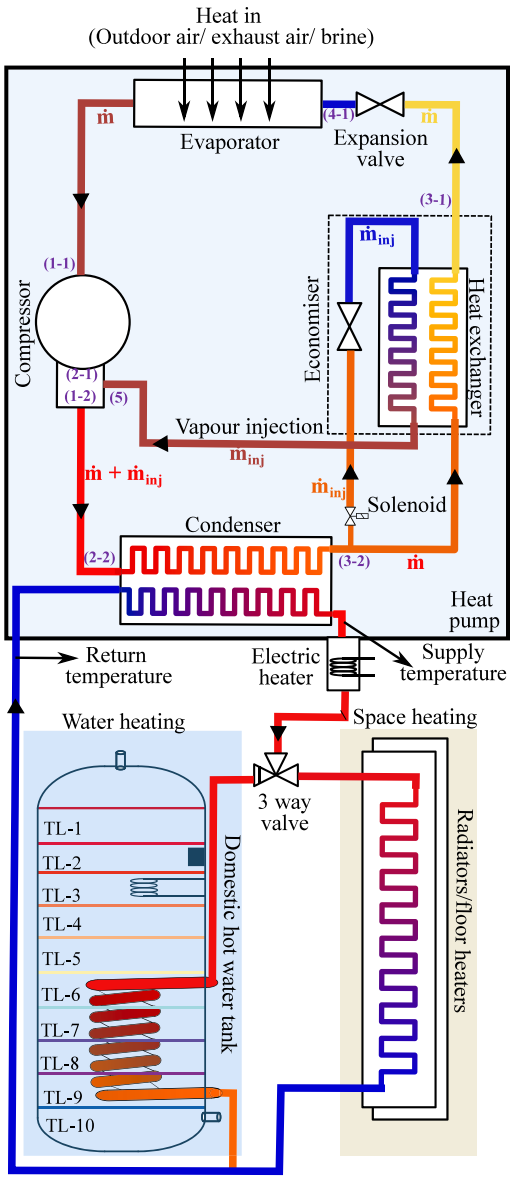

Fig. 1. Heating system in typical single family houses. 3-way valve helps in directing the heating to either the water tank or radiators. TL represents the temperature in 10 different portions of the tank.

- The specific enthalpy at state 1–2, 'h_{1-2}' is obtained by using the energy balance equation at vapour injection port of the compressor and is given by

$$\dot{m}_{inj}(h_{1-2} - h_5) = \dot{m}(h_{2-1} - h_{1-2})$$
$$h_{1-2} = \frac{\dot{m}h_{2-1} + \dot{m}_{inj}h_5}{(\dot{m} + \dot{m}_{inj})} \tag{2}$$

- The electric power consumed by the compressor is found as

$$P_{comp} = \frac{\dot{m}(h_{2-1} - h_{1-1}) + (\dot{m} + \dot{m}_{inj})(h_{2-2} - h_{1-2})}{\eta_{isent}} \tag{3}$$

where, η_{isent} is the isentropic efficiency. The variation in isentropic efficiency during various operating conditions is obtained as described in [31].

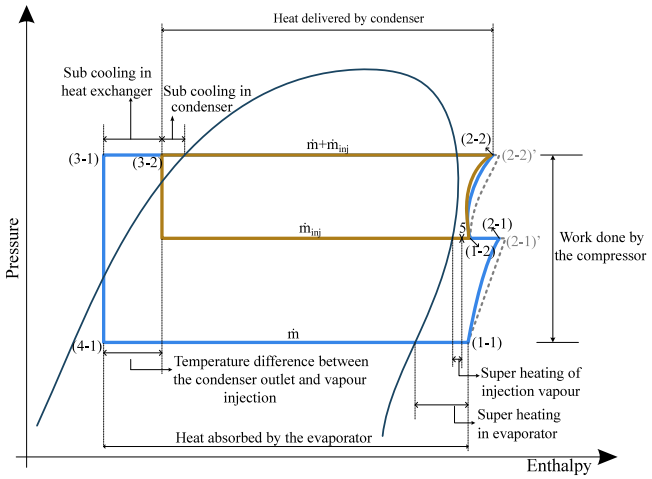

Fig. 2. Vapour compression heat pump cycle with vapour injection [29].

- The COP of a heat pump is expressed as

$$COP = \frac{(\dot{m} + \dot{m}_{inj})(h_{2-2} - h_{3-2})}{P_{comp}} \tag{4}$$

2.3. Indoor temperature estimation

The natural ventilation rate is the continuous air exchange rate of the indoor air with the outdoor air, to ensure good indoor air quality. Infiltration corresponds to air leakage into or out of a building through cracks, gaps, and openings in the building envelope [32]. As warm indoor air is exchanged with cold outdoor air, there is heat loss both due to natural ventilation and infiltration. If natural ventilation is controlled, then some amount of ventilation heat loss can be recovered through a heat recovery unit.

With this context, the detailed procedure for estimating indoor temperature is described in [6]. A brief summary of the procedure is listed below.

- The heat transfer coefficient of a house's envelope 'U_{value}', based on the construction materials is obtained. This is followed by the calculation of heat loss due to infiltration and natural ventilation. The heat recovery of ventilation losses by a heat recovery unit is also taken into account. Finally, considering all these aspects of heat losses, the total heat transfer coefficient is determined. The reciprocal of the total heat transfer coefficient gives the value of the thermal resistance of the house.
- The thermal mass of the house is determined on the basis of the value of the time constant obtained for typical houses.
- Finally, indoor temperature is estimated using a resistance–capacitance network. Here, the resistance corresponds to the thermal resistance and the capacitance to correspond to the thermal mass of the house. The inputs to this model are the heat provided by the heat pump via heat emitters modelled as a current source. Another input is the outdoor ambient temperature modelled as a voltage source.
- The water heated by the heat pump is supplied to the heat emitters, i.e., radiators or floor heating. Based on the indoor temperature, followed by the supply and return temperature of water in the heat emitters, the thermal output is computed.

2.4. Water temperature estimation in a domestic hot water tank considering stratification

The domestic hot water tank is stratified. The control action for the water heating by the heat pump depends on the location of the temperature sensor in the tank. Hence, to estimate the temperature at different locations in the hot water tank, the water tank is assumed to be divided into 10 equal volumes, which would be further referred to as layers in this article. This is shown in Fig. 1.

In the domestic hot water tank, the temperature sensor is assumed to be placed in layer 2. The electric heater and the hot water coil are assumed to be present in layer 3 and between layers 6 and 9 respectively. The water heated by the heat pump is passed through the coil immersed in the tank. The heat released by the coil is used to heat the water in the tank. Hot water is extracted from the top and is replaced by an equal volume of cold water at the bottom of the tank.

The temperature of the water at different locations is estimated through a state–space model, considering heating from the hot water coil and the electric heater. Furthermore, heat transfer between different layers due to conduction, hot water extraction, and inversion mixing is also taken into account. In addition, heat loss from the tank to the surrounding in which it is placed is also considered. The detailed mathematical model for estimating the temperature at different locations in the tank is described in [33].

2.5. Physics-based model for estimating the electricity consumption by heat pumps in single-family houses

The integrated physics-based model that involve the heat pump, space and water heating systems, to estimate the electric power consumption, is shown in Fig. 3.

Depending on whether the heat pump provides space or water heating, the difference between the actual and reference temperature values is fed into the appropriate PI controller. The controller provides an estimate of heat '$Q_{heat}{}^{**}$' required to maintain the desired temperature.

Since the control action for water heating is based on the location of the temperature sensor, the temperature of the water in layer 2, '$T_{water,TLp}$' is considered. The detailed procedure for designing the space and water heating controller is described in [30].

The thermal output from the heat emitters at different water supply and return temperatures, during various indoor temperatures, are implemented in look-up tables. These tables provide estimates of water supply and return temperatures, at a specific indoor temperature 'T_{room}' to deliver the desired heat value '$Q_{heat}{}^{**}$'. If there is any limitation in the heat delivering capability of the heat emitters, '$Q_{heat}{}^{**}$' would be limited. The heat provided by the heat emitters considering the limitation is represented by '$Q_{heat}{}^{*}$'.

A similar procedure is adopted to obtain the estimates of the supply and return temperature of water in the hot water coil to deliver the desired value of heat. As the hot water coil is placed between layers 6 and 9, an average value of water temperature '$T_{water,average}$' is taken into account in the respective layers.

Based on the estimated supply temperature of the water obtained from a specific lookup table and the actual return temperature of the water, the required condenser temperature is estimated. Furthermore, using the estimated condenser temperature, the source temperature 'T_{source}' of the heat pump and the heat demanded '$Q_{heat}{}^{*}$', the heat pump model provides the heat output 'Q_{heat}', the corresponding compressor speed, and information on the actual consumption of electric power by the heat pump, including the use of direct electric heating.

3. Parameter description

3.1. Heat pump parameters

Scroll compressors are commonly used in residential applications. Hence, the compressor in a heat pump is assumed to be equipped with a 'ZPV030' Copeland's variable speed scroll compressor, having an electrical rating of 3 kW. The compressor displacement volume is 30 $\left(\frac{\text{cc}}{\text{rev}}\right)$ and the operating envelope is shown in Fig. 4. The refrigerant

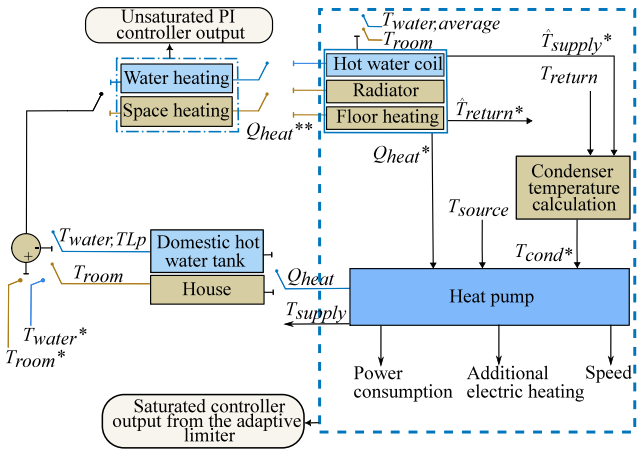

Fig. 3. Integrated physics-based model for estimating the electricity consumption in heating systems [30].

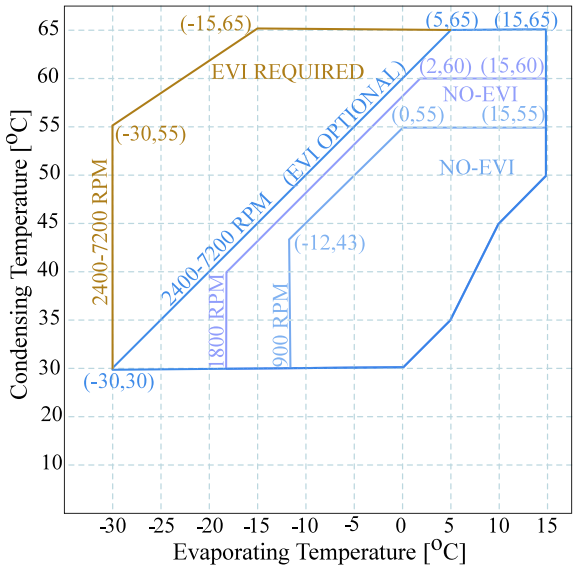

Fig. 4. Compressor operating envelope [28].

Table 1
Temperature drop between source and evaporator.

Type of heat pump	Source temperature	Temperature drop (° C)
Ground source	Ground	10
Air to water	Outdoor ambient air	8
Exhaust air	Indoor air	20

'R410a' is used. The rating of the electric heater present before the 3-way valve in Fig. 1 is 3 kW.

Based on the Refs. [34,35], the temperature drop set between the source and the evaporator is shown in Table 1. The ground temperature is chosen to be 10 °C.

3.2. Building parameters

The heat transfer coefficient 'U_{value}' of single-family houses in Sweden, according to the year of construction, is obtained from Ref. [36]. Following a conservative approach, houses constructed before 1961 are excluded as the source for heating is very mixed. For example, they could be heated with wood, oil, direct electric heating, or heat pumps, and thus the source of the heating is unclear.

The thermal properties of the houses together with the type of heat pump, the type of heat emitter, and the number of houses considered for the analysis are shown in Table 2. In this study a natural ventilation rate of 0.35 $\left(\frac{l}{s \cdot m^2}\right)$ is used.

The southern half of Sweden is chosen as the geographical boundary, as most of the inhabitants live in this region [37]. The average size of a Swedish single-family houses is 122 m^2 [38] and the same is considered. The indoor temperature is set to be 20 °C [39].

3.3. Parameters of the domestic hot water tank

The thermal and physical properties of the hot water tank used in this study are shown in Table 3 [41]. Based on [42], a heat transfer coefficient of 450 $\frac{W}{m^2 K}$ is used for the water coil. Furthermore, considering a coil of 35 m length with an external diameter of 0.03 m, the heat transfer coefficient of 1484 $\frac{W}{K}$ is obtained for the water coil.

The average domestic hot water consumption profile for a day, based on time diaries is obtained from [43], which describes the hot water consumption profiles in Swedish single-family houses. The average number of people living in Swedish single-family houses is 2.7 [44] and the same is considered for the analysis.

3.4. Modified Nordic-32 bus system

The original Nordic-32 bus system [45,46] is a fictitious system with similarities to the actual Swedish power system. Furthermore, this is a downscaled version of the actual Swedish power system. It is important to mention that this system is heavily loaded, as it was primarily designed to study voltage instability. As one of the objectives of this article is to study frequency support, using flexibility from single-family house heating systems, the loading is taken to be 70% of the original case (7.74 GW). Furthermore, the water time constant in the hydro turbine governor models is set to 1.5 s, which is typical in Sweden [47] (In the original system, this value was 1 s).

A future case with an almost sustainable power production is considered. Thus, fossil fuel and nuclear power plants in the central and southern regions have been replaced by wind power plants except for generator G15. This is shown in Fig. 5. The models 'REGCBU1' and 'REECDU1' are used for the converter and electrical control modules in the wind power plants. The parameter settings of these models are based on the typical range given in [48]. Active power support from wind power plants to arrest the initial frequency fall is not taken into account as they cause a second frequency drop [49]. Thus, wind power plants provide only reactive power support during disturbances [50] and no active power support is assumed.

Furthermore, to account for the impact of the increase in power-electronic interface loads, the load characteristics are changed to 60% constant power load and 40% constant current load for active power (originally constant current). The load characteristics for reactive power are changed to 60% constant power load and 40% constant impedance load (Originally constant impedance). Finally, the rating of the G8 hydro generator is changed to 1000 MVA, with active power scheduled at 950 MW, and it is the loss of this unit that is investigated.

3.5. Case study description

In the current study, the flexibility is quantified for outdoor ambient temperatures varying between −10 °C and 10 °C, as this represents typical autumn–winter–spring situations in the Nordics [51]. The indoor temperature and the water temperature in the tank are set to be 20 °C and 55 °C respectively, during normal conditions.

The interview study revealing the willingness of residents to compromise thermal comfort in the event of a major power crisis to avoid blackouts exists [6]. Thus, based on the interviews, the flexibility potential is estimated by reducing the indoor temperature from 20 °C to 18 °C, 17 °C, 16 °C and 15 °C respectively. Correspondingly, the

Table 2
Parameters considered for thermal modelling of building [36,37,40].

Year of construction	U_{value} ($\frac{W}{m^2K}$)	Time constant (Hours)	Infiltration ($\frac{l}{s\ m^2}$)	Efficiency of Heat recovery	Heat emitter	Type of heat pump	Number of houses (in Million)
1961–1975	1.4	34.0	0.00	0.00	Radiators	Ground source	0.4455
1976–1985	0.9	38.0[a]	0.60	0.60	Radiators	Air to water	0.2743
1986–1995	0.9	42.0[a]	0.00	0.60	Radiators	Air to water	0.1474
1996–2009	0.8	48.0[a]	0.00	0.00	Floor heating	Exhaust air	0.1056
2010-beyond	0.7	53.0	0.80	0.00	Floor heating	Exhaust air	0.1122

[a] Interpolated.

Table 3
Parameters of domestic hot water tank model [33].

Parameter	Value
Volume	180 L
Heat conduction co-efficient of tank per layer (U_i)	0.187 $\frac{W}{K}$
Electric heater	3000 W
Thermal conductivity of water (K_i)	2.21 $\frac{W}{K}$
Specific heat capacity of water (C_p)	4180 $\frac{J}{Kg\ K}$
Heat transfer coefficient of the water coil ($U_{watercoil}$)	1484 $\frac{W}{K}$

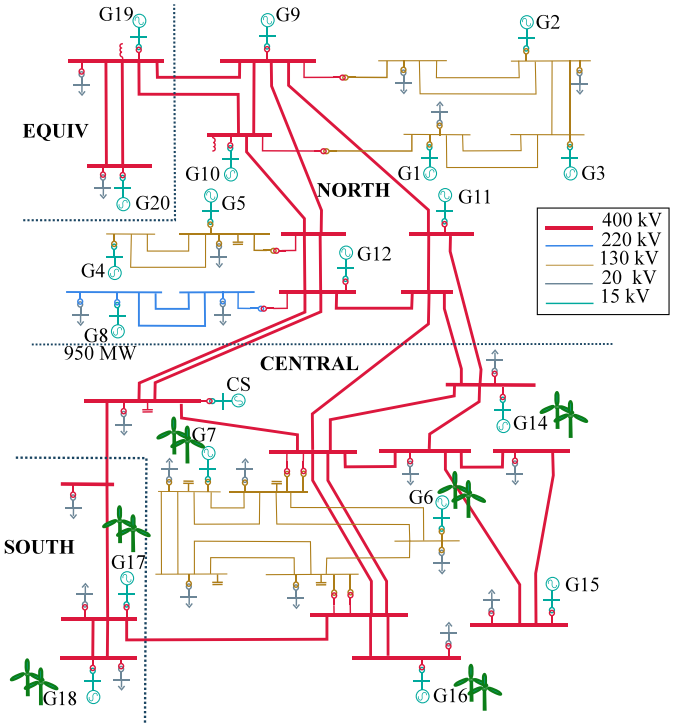

Fig. 5. Modified Nordic-32 bus system.

water temperature in the tank is reduced from 55 °C to 50 °C, 48 °C, 46 °C, and 44 °C respectively.

A range of minimum acceptable temperatures for space and water heating is used, as opposed to a single value. This helps in obtaining a range of flexibility levels as opposed to a single value.

At hour 6.75, an event occurs in the power system that requires emergency power support, and thus the reference temperatures for space and water heating are reduced to support the grid. The recovery period begins at hour 24 and the objective is to recover the indoor temperature within a period of 24 h.

The set-point changes for space and water heating are realistic control implementations. For instance, there are companies already in operation such as NGENIC and Tibber which helps in reducing the electricity consumption based on hourly electricity prices using heat pumps for numerous customers.

3.6. Delimitations

The following are the delimitations of the current study:

- The thermal thresholds for quantifying flexibility is based on qualitative interviews conducted in the southern half of Sweden. This study provided a deep understanding of the thermal comfort of households and their perspectives on offering flexibility. Consequently, statistical generalisations are not possible using a quantitative method such as survey [6].
- With the objective of keeping the result derivation 'clear and easily reproducible,' in light of detailed knowledge, deterministic models are used to quantify the aggregated flexibility of a million houses. However, it is important to state that five different typical houses equipped with different types of heat pump are considered. Furthermore, a range of minimum acceptable indoor temperatures stated in interviews is used for flexibility quantification. This helps in obtaining a range of flexibility levels as opposed to a single value.
  Using the available data on thermal thresholds and typical thermal properties of houses for simulations, can help reflect common operating conditions during different degrees of thermal compromise at various outdoor ambient temperatures. Hence, employing a deterministic approach in this case is beneficial.
- Experimental validation of the models developed is not included.

4. Terms used for flexibility quantification

Flexibility is quantified in terms of an instantaneous reduction in power and the corresponding duration with respect to normal conditions. A reduction in electric energy during the flexibility period and a net reduction in electric energy considering the recovery period with respect to the normal condition are also quantified. This is shown in Fig. 6. The period of time during which the temperatures start to reset to normal conditions is referred to as the recovery period.

5. Results and discussion

5.1. Heat pump

The heat pump model is validated by comparing the results obtained under standard air conditioning and refrigeration institute conditions i.e., 7.2 °C evaporator temperature, 54.4 °C condenser temperature, with super heating of 11 °C and sub-cooling of 8.3 °C, with the data given in [28].

The results are tabulated in Table 4 and the agreement is good. A discrepancy of 6.7% is observed in the heat delivered. This might be because the heat losses in the evaporator are not accounted for. However, the results of the electric power consumption from the model presented agree well with the data provided in [28].

The performance of an air source heat pump during EVI operation is shown in Fig. 7. Higher condenser temperatures can be achieved

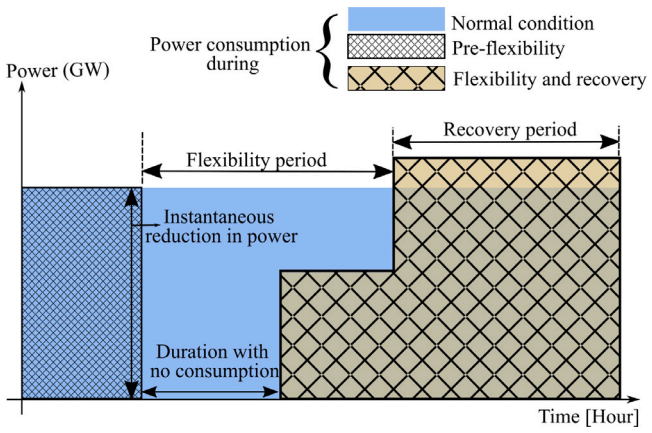

Fig. 6. Terms used for flexibility quantification.

Table 4
Comparison of result obtained with data provided in [28].

Compressor model	ZPV030	
	Given	Obtained
Speed (RPM)	3600	3600
Rated Capacity (kW) @ ARI 3600 RPM	9.7	10.35
Electric power input (kW)	2.98	2.94
COP (W/W)	3.25	3.52

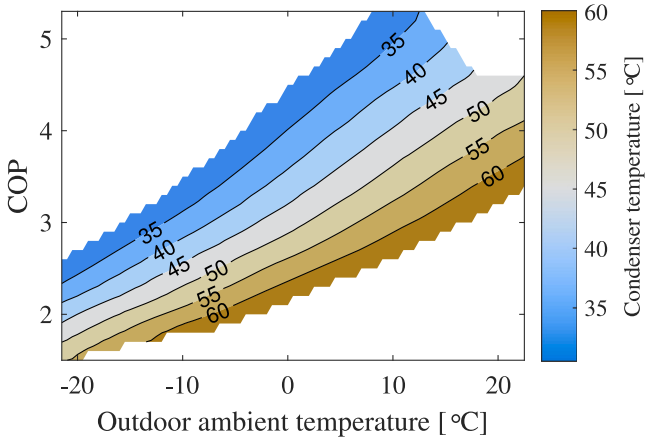

Fig. 7. Condenser temperature as a function COP and outdoor ambient temperature for an air source heat pump with EVI technology.

with this mode, in particular at low ambient temperatures as opposed to operating in the non-EVI mode [6]. The water supply temperature depends on whether the heat pump provides space or water heating. Furthermore, in space heating, it depends on the type of heating, that is, floor heating or radiator heating. This means that the condenser temperature should be higher than the desired water supply temperature.

As the outdoor ambient temperature falls, the COP also reduces accordingly, resulting in an increase in the electric power consumption. This is important since, typically it is under very cold conditions that the power system could be operated with small margins.

From the representation point of view, water supply temperatures of 60 °C, 45 °C and 30 °C are selected. The COP as a function of the heat delivered and outdoor ambient temperature, during above conditions is shown in Fig. 8. The heat delivering capacity increases with an increase in the outdoor ambient temperature. Furthermore, for a given outdoor ambient temperature, the heat delivering capability increases when the water supply temperature is reduced.

5.2. Performance comparison between a fixed speed and a variable speed, air to water heat pump

A house constructed during 1976–1985 with the properties discussed in Table 2, is equipped with an FSHP dealt with in [15], in one case. In the second case, it is assumed that the same house is equipped with a VSHP, discussed in Section 5.1. An outdoor ambient temperature of −10 °C is assumed.

The performance comparison between an FSHP and an VSHP, when the reference indoor temperature is at 20 °C and when changed to 17 °C, is shown in Fig. 9. Fig. 9(a) and 9(d) show that the indoor temperature can be accurately maintained at 20 °C, when equipped with a VSHP rather than an FSHP. This is because the heat delivered by a VSHP can be modulated according to the requirements by modulating the speed of the heat pump. As a result, the heat pump does not need to be turned on and off, as in the case of a FSHP. This can be observed in Fig. 9(b), 9(e) and 9(c), 9(f). As a result, although the temperature of the water supplied is the same in both cases, the average electric power consumption is 19% higher in FSHP compared to VSHP.

When the reference value of the indoor temperature is changed to 17° C, the electrical power consumption of both heat pumps is zero, until the indoor temperature reaches close to the reference value. In case of a VSHP, the electric power consumption reduces as the indoor temperature reduces. However, this is not the case for an FSHP. The electric power consumption remains the same as while maintaining the indoor temperature at 20 °C. This comparison shows that flexibility quantification in terms of power would be higher for FSHPs compared to VSHPs.

Thus, a very important conclusion is that since VSHPs are expected to take over in the future, the flexibility potential will be overestimated if FSHPs are used in these types of study.

5.3. Flexibility analysis of a typical house constructed during 1976–1985 at an outdoor ambient temperature of −10 °C

The thermodynamics in the house while providing flexibility, by reducing the indoor temperature to 17 °C and the water temperature in the tank to 48 °C is shown in Fig. 10. Before changing the reference temperatures, it is observed in Fig. 10(b), that the indoor temperature is not exactly maintained at 20 °C, although a VSHP is used. This is because the VSHP can only provide space or water heating at a time. When the VSHP is in water heating mode, there is a slight drop in indoor temperature compared to the reference value, and this is seen in Figs. 10(a), 10(b), and 10(c). In Fig. 10(c), it is observed that there is a spike in the condenser temperature, supply, and return temperature of water during the water heating mode, as higher temperatures are required for heat transfer.

Furthermore, it is observed that the water temperature in the tank is not uniform as a stratified model of a domestic hot water tank is considered. All layers in the tank follow a similar trend except for the temperature in layer ‘TL-10’, since cold water enters this layer every time hot water is extracted. Additionally, there is no heating element in this layer. The period of time during which there is no withdrawal of hot water (at night between 0 and 4 h), temperature ‘TL-10’ increases mainly because of heat transfer from the top layers in the tank, and accordingly the temperature of the water in the top layers reduces.

When the reference temperature of space and water heating is reduced at hour 6.75, there is no electric power consumption for nearly 3.2 h, due to the thermal inertia of the building and the hot water tank. This can be seen in Fig. 10(d). Furthermore, it is observed that there is no water heating provided as the temperature in layer ‘TL-2’ is above the reference temperature, although the temperature of water is lower in the subsequent layers. This shows the significance of using a stratified model for a domestic hot water tank in flexibility studies. Thus, the house provides a flexibility of 2.68 kW, in terms of an instantaneous reduction in power for nearly 3.2 h.

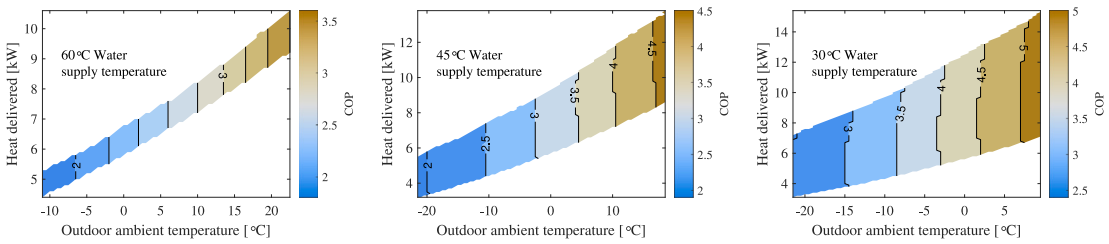

(a) Supply temperature of water at 60°C (b) Supply temperature of water at 45°C (c) Supply temperature of water at 30°C

Fig. 8. Heat delivering capability of an air source heat pump with EVI technology, while supplying water at 60 °C, 45 °C and 30 °C.

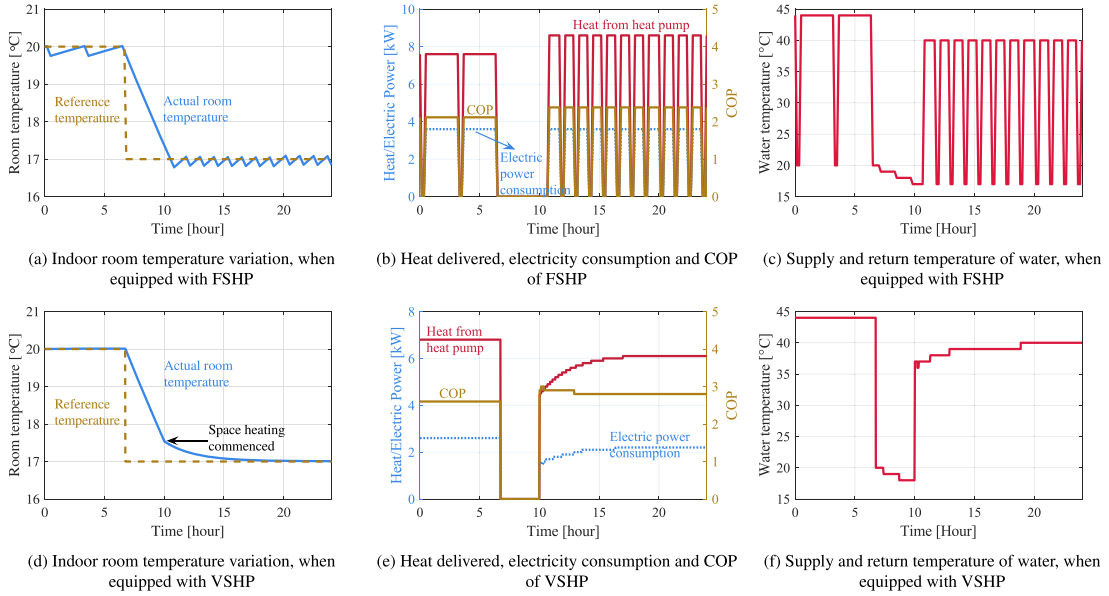

(a) Indoor room temperature variation, when equipped with FSHP (b) Heat delivered, electricity consumption and COP of FSHP (c) Supply and return temperature of water, when equipped with FSHP

(d) Indoor room temperature variation, when equipped with VSHP (e) Heat delivered, electricity consumption and COP of VSHP (f) Supply and return temperature of water, when equipped with VSHP

Fig. 9. Performance comparison between a fixed and a variable speed heat pump.

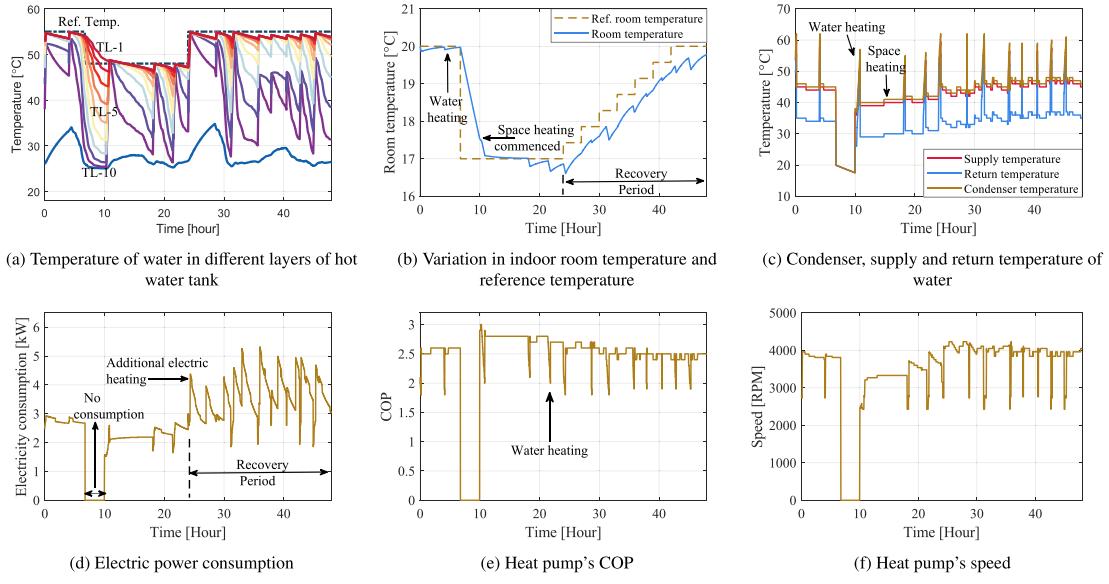

(a) Temperature of water in different layers of hot water tank (b) Variation in indoor room temperature and reference temperature (c) Condenser, supply and return temperature of water

(d) Electric power consumption (e) Heat pump's COP (f) Heat pump's speed

Fig. 10. Thermodynamics in the house constructed during 1976–1985 equipped with the air-source heat pump with vapour injection technology, at an outdoor ambient temperature of −10 °C.

After 3.2 h, the VSHP starts again to maintain the temperature at the reference level. It is observed that the supply temperature of the water is reduced when the reference temperatures for space and water heating are reduced. Furthermore, in Fig. 10(e), it is seen that COP reduces with increasing condenser temperature because the compressor has to do more work and this is evident especially during water heating. The speed of the VSHP corresponding to the COP is shown in Fig. 10(f). Compared to the normal condition, the electric energy consumption is

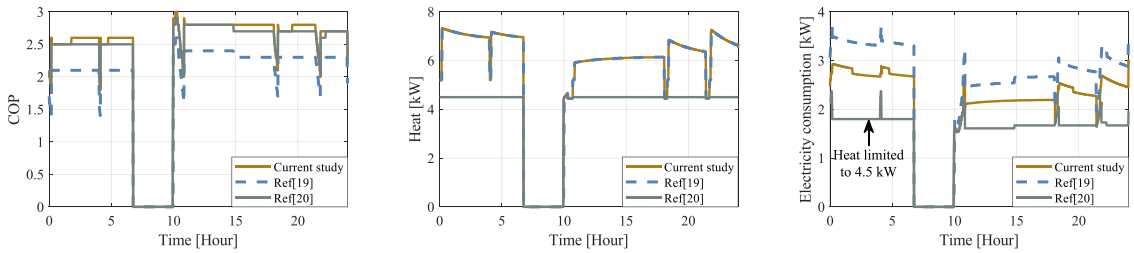

(a) Comparison of COP (b) Comparison of heat delivered (c) Comparison of electricity consumption

Fig. 11. Comparison of COP, heat delivered and electricity consumption by the heat pump in the study with [19,20].

20 kWh lower during the flexibility period starting from hour 6.75 until hour 24.

An important aspect to account for is the power needed to restore the situation to the 'fully normal state. During the recovery period, if the objective is to limit electric power and energy consumption, while restoring the indoor temperature to 20 °C, the reference temperature should preferably be increased in steps. The reason is that, at an outdoor ambient temperature of −10 °C, the heat delivering capability is lower, as seen in Fig. 8. Thus, if there is a higher heating requirement, additional electric heating must be used. However, despite gradually increasing the reference temperature, additional electric heating is used as seen in Fig. 10(d). However, in this case, the peak value of the power consumed is lower, compared to the case when the reference temperature is increased directly to 20 °C.

Until the beginning of the recovery period, the electric energy consumption is 20 kWh lower compared to the normal condition. During the recovery period, the electric energy consumption is 16.48 kWh higher than in normal condition. Thus, the net reduction is around 3.5 kWh.

In the above case, if the reference temperature is directly increased to 20 °C, an additional electric energy of 11.5 kWh occurs with respect to the normal condition and instead of energy savings, energy loss is obtained.

The reference temperature for water heating is not increased in steps because the heating energy requirements are not as high compared to space heating.

5.4. Comparison of the heat pump's performance in the current study with empirical models of variable speed heat pumps

Fig. 11(a) and 11(c) show the comparison of COP and electric power consumption of the air to water VSHP studied in Section 5.3 (excluding the recovery period) with respect to the empirical models described in [19,20]. Empirical models are based on outdoor ambient temperatures and water supply temperatures. However, it should be noted that the heat pump parameters described in Section 3.1 are missing in empirical models.

It is observed that the COP obtained from [20], matches well with the current study, as opposed to the COP obtained from [19]. However, while looking at the electric power consumed, it is observed that the actual consumption in [20] is lower compared to the current study, as the heat delivering capability at an outdoor ambient temperature of −10 °C is limited to 4.5 kW. This can be seen in Fig. 11(b) and 11(c). The reason for the limitation in the heat delivering capability [20] and the COP values obtained from the empirical models used in [19,20] are unknown.

Thus, using physics-based models makes flexibility quantification clear and transparent as opposed to empirical modelling.

5.5. Flexibility quantification

Flexibility is analysed and quantified for all houses described in Section 3.2, by reducing the temperatures of space and water heating. The quantification of flexibility at the individual house level is shown in Table 5. As expected, the flexibility potential in terms of power is observed to be higher in houses that are less energy efficient. Among the houses constructed during 1996 and 2010, the latter has a high value of flexible power due to high infiltration loss. Also, among the houses constructed during 1961 and 1976, the latter has a high value of flexible power, as it is equipped with an air-to-water heat pump, which is less efficient compared to the ground source heat pump.

In all the categories of houses under study, a positive net reduction in electric energy is witnessed. The reduction in electric energy during the flexibility period increases with an increase in the degree of thermal compromise. However, the net reduction in electric energy depends on the electric energy consumption during the recovery period. In the case of houses, where the utilisation of direct electric heating is lower during the recovery period, the net reduction in electric energy increases with a higher compromise in thermal comfort, for instance, in houses constructed during 1986–2009. In contrast, if there is a higher utilisation of direct electric heating, for instance, in houses constructed during 1976, the net reduction in electric energy decreases with an increase in the compromise of thermal comfort. Thus, the net reduction in electric energy in a specific house category during different degrees of thermal compromise varies from case to case.

The average electric power consumption on a system level, during pre-flexibility, flexibility and the recovery period, respectively, for two example cases with respect to the normal condition, at an outdoor ambient temperature of −10 °C is shown in Fig. 12. During the flexibility period, the average consumption is obtained from the instant the electric power consumption starts until the end of the recovery period. The average consumption is considered due to the aggregation effect of one million houses. These plots serve as valuable information for power balancing.

As anticipated, it is observed that the duration of time without electric power consumption increases with an increase in the reduction of temperatures for space and water heating. The same holds true when considering the total reduction in electric power consumption while offering flexibility. The average consumption of electric power during the recovery period increases in cases with a higher reduction in temperature during the flexibility period. This is because the amount of work done by the heat pump, when increasing the indoor and water temperatures to the set reference temperatures within a period of 24 h, is higher in the above case. However, flexibility in terms of an instantaneous reduction in power is the same in all cases and is independent of the reference temperatures set for space and water heating during the flexibility period.

5.6. Mathematical validation of the models developed

For mathematical validation of the models developed, the results obtained from Sections 5.2 and 5.3 will be used as a basis for comparing the thermal model of the house and the thermal model of the domestic hot water tank.

Table 5
Flexibility quantification in the houses under study.

Construction year of house	Electric energy reduction (kWh) including recovery period, at an outdoor ambient temperature of −10 °C				Flexibility (kW)
	SH:18 °C, WH: 50 °C	SH:17 °C, WH: 48 °C	SH:16 °C, WH: 46 °C	SH:15 °C, WH: 44 °C	
1961–1975	3.9	6.1	5.9	6.1	1.8
1976–1985	3.8	3.5	2.8	0.7	2.7
1986–1995	4.0	6.1	7.3	8.2	1.6
1996–2009	0.8	1.5	2.3	3.0	1.0
2010- beyond	1.3	2.4	2.8	0.7	1.6

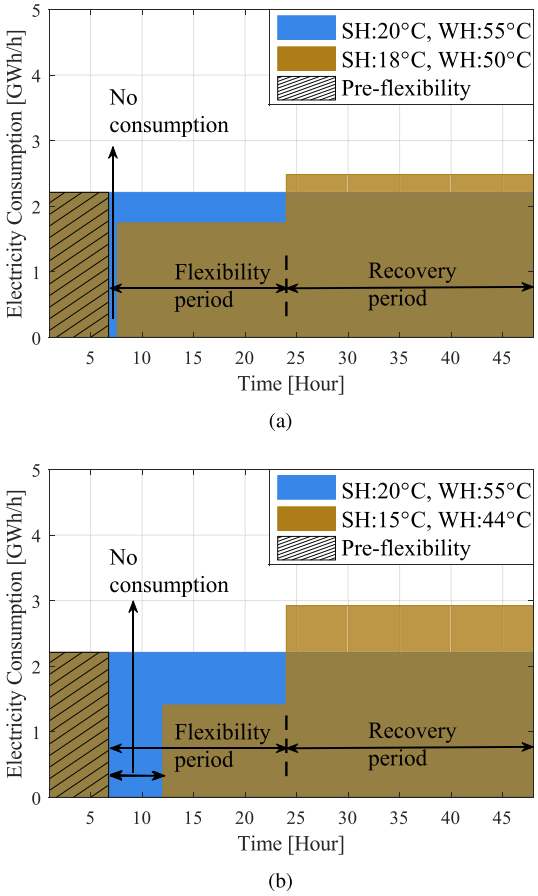

Fig. 12. Electricity consumption during different set point temperatures at an outdoor ambient temperature of −10 °C. (SH:Space heating, WH: Water heating).

5.6.1. Validation of the thermal model of the house

The total U_{value} of the house considering infiltration, natural ventilation, and heat recovery is estimated at 227.93 $\frac{W}{K}$. Hence, to maintain an indoor temperature of 20 °C and 17 °C, at an outdoor ambient temperature of −10 °C, the heat requirement is 6.8 kW and 6.15 kW, respectively. This matches well with the result presented in Fig. 9(d) and 9(e).

Furthermore, the empirical model defined in [20] to estimate the temperature of the water supply in the radiators is given by

$$T_{set,supply} = 36.67 - 0.78\ T_{amb} - 0.0040\ T_{amb}^2 \quad (5)$$

Here, T_{amb} refers to the outdoor ambient temperature. According to this empirical model, the water supply temperature is 44 °C and this matches well with the simulation results obtained in Fig. 9(f). Thus, the thermal model of the house works as expected.

5.6.2. Validation of the domestic hot water tank

The time constant of the domestic hot water tank, considering the thermal mass of water and the thermal resistance of the tank in Table 3 is estimated to be 111.76 h. As discussed in Section 5.3, there is no water heating or water withdrawal between 0.2 and 4 h, and the indoor temperature is near 20 °C. During this period, using Newton's law of cooling, the average temperature of the water is estimated to fall from initial 51.3 °C to 50.25 °C. Comparing this result with Fig. 10(a), it is observed that the hand calculations match with the simulation results. Thus, the model works as intended.

5.7. Flexibility quantification during different conditions

The results from flexibility analysis with respect to the normal case, for different temperatures set for space and water heating are consolidated and shown in Fig. 13.

In Fig. 13(a), it is seen that during the normal case, the electric energy consumption for space and water heating is reduced with increasing outdoor ambient temperature. Consequently, the amount of flexibility that can be offered in terms of instantaneous reduction in power is reduced.

As explained earlier, the reduction in electric energy during the flexibility period increases with an increase in the degree of thermal compromise. At the system level, this also holds for the net reduction in electric energy, including the recovery period. This is observed in Fig. 13(b).

The duration of time without electric power consumption during the flexibility period, for various degrees of thermal compromise, at outdoor ambient temperatures ranging between −10 °C and 10 °C is shown in Fig. 13(c). The flexibility in terms of an instantaneous reduction in electric power is also shown in this figure. It is observed that the flexibility in terms of an instantaneous reduction in electric power is independent of the degree of thermal compromise. However, the duration for which this flexibility can be offered increases with an increase in the degree of thermal compromise.

According to data in [52] and Fig. 13(c), it is inferred that from the perspective of endurance and flexibility volume, single-family houses in Sweden have the potential to act as virtual power plants for a short period.

5.8. The role of flexibility in limiting the instantaneous frequency deviation during loss of a major generating unit

The instantaneous value of the flexibility potential, at an outdoor ambient temperature of −10 °C, is estimated to be 2.1 GW. This is obtained by summing up the total flexibility from the houses built after the 1960's in the southern half of Sweden, representing 54% of the total single-family houses.

As the Nordic-32 bus system is a down-scaled version of the actual Swedish power system, the flexibility also needs to be scaled down accordingly. The peak demand in Sweden during the years 2022–2023 was 25 GW and the peak load in the modified Nordic-32 bus system is 7.74 GW. The corresponding flexibility level for this modified test system would be approximately 650 MW, which is about 8.4% of the total load in the system.

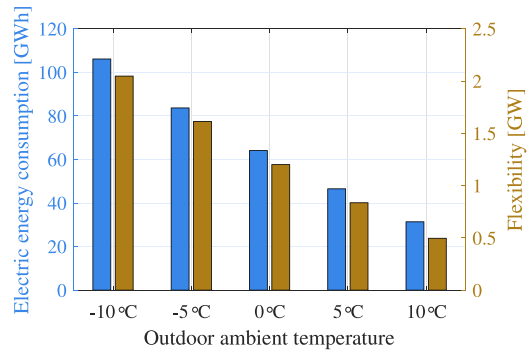

(a) Energy consumption for normal case and flexibility

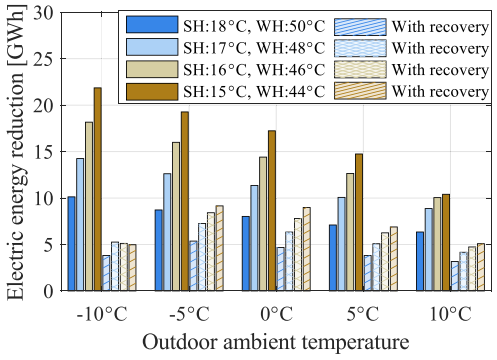

(b) Electric energy reduction.

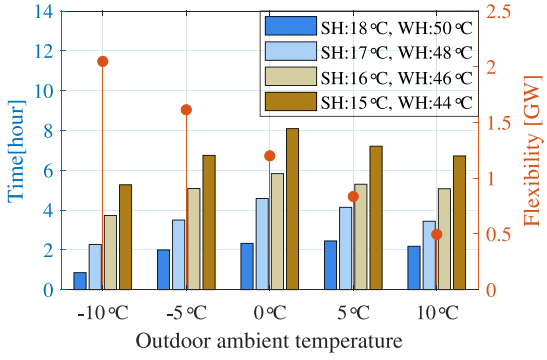

(c) Duration of time with zero electric power consumption

Fig. 13. Consolidated results from flexibility analysis. (SH:Space heating, WH: Water heating).

In the modified Nordic-32 bus system explained in Section 3.4, during the loss of the generating unit G8, producing 950 MW, the frequency deviation reaches below 48 Hz as seen in Fig. 14. To study the impact of flexibility in improving frequency nadir, it is assumed that local frequency sensors with a filter time constant of 0.1 $\frac{sec}{rad}$ are present in all heat pumps. The heat pumps are disconnected from the power supply when a frequency of 49.5 Hz is sensed. The impact of flexibility at different levels, ranging from 50% to 100% on the frequency nadir, is shown in Fig. 14. It is observed that by using at least 70% of the estimated flexibility, it is possible to limit the frequency nadir to stay above 48.8 Hz, else the under-frequency load shedding scheme is triggered. 70% of the estimated flexibility corresponds to about 5.9% of the total load in the system.

For comparison, a case where wind turbines are assigned to cover 90% flexibility is also included in Fig. 14, it is assumed that wind conditions allow this. Active power support (power shaping) from wind power plants during the loss of a major generating unit is based

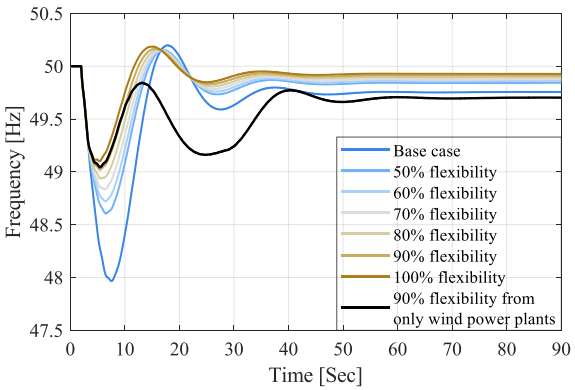

Fig. 14. Impact of flexibility on frequency nadir.

on articles [53,54]. Compared to normal operating conditions, active power support of about 600 MW is considered for 5 s. Later, active power production gradually decreased to −200 MW in 20 s, compared to normal operating conditions.

In Fig. 14, it is quite clear that the active power support of the wind power plants is for the initial 14 s of the disturbance period. Thus, the instantaneous frequency deviation is limited to 49 Hz as in the case with provision of 90% flexibility from the buildings.

However, after sometime since the turbines have to recover the rotational energy borrowed from the grid, there is a 800 MW deficit that must be found during the first minute, which is not the case with the buildings. Consequently, a second frequency drop is observed, as demonstrated in [49]. Furthermore, the steady-state frequency deviation with active power support from houses equipped with heat pumps is lower compared to active power support from wind power plants. This is observed in Fig. 14.

In the future, one could also imagine that wind turbines operated at over-speed and thus could emit this ‘over-speed energy’ during approximately 20 s. Another possibility, in a future with a very large number of wind turbines, could be operating wind turbines with de-rated power prepared to take on a power deficit condition, but the energy loss for continuously providing this possibility would be very high.

5.9. Future work

Two valuable further efforts for future work are

- Experimental validation of the proposed integrated model that involves a heat pump, a space and water heating system in a real house. This helps in providing deeper insights that are not captured by simulations.
- Employing stochastic models to quantify flexibility in one million houses, to account for the uncertainty in the buildings’ thermal properties and indoor temperature set points based on the occupants behaviour.

6. Conclusion

In this article, large scale power grid resilience reinforcement from single-family houses equipped with heat pumps, to a transmission grid encountering disruptive events is studied. A flexible physics-based model of a heat pump is developed to obtain the electricity consumption under various operating conditions considering operational limitations. This is a reproducible and adaptable physics-based model that is not data-demanding and can be conveniently adapted to any operational condition. In addition, an integrated model is developed

that involves detailed representations of the heat pump, space heating, and water heating to estimate the consumption of electricity under various operating conditions.

It is shown that the flexibility potential will be overestimated if fixed-speed heat pumps are used in these types of studies. In addition to this, it is also shown that using physics-based models makes flexibility quantification transparent and clear compared to empirical models. Furthermore, this study reveals that slow recovery aids in energy savings by gradually increasing the reference temperature for space heating, to minimise the use of direct electric heating.

The houses built after the 1960s in the southern half of Sweden, representing 54% of the total single-family houses, are considered for the analysis. For the power system with a dimensioning fault of 1.45 GW, the flexibility level found range between 2.1 GW and 0.5 GW, for outdoor ambient temperatures varying between −10 °C and 10 °C respectively. These estimates are independent of the degree of thermal compromise. However, the duration for which the above flexibility values can be provided is dependent on the degree of thermal compromise.

By reducing indoor and water temperatures from 20 °C and 55 °C, to 15 °C and 44 °C, the power system can be relieved with 2.1 GW for 5 h and 0.8 GW for the next 12 h, at −10 °C outdoor temperature. As a consequence of offering flexibility, the average electric power consumption increases to 2.9 GW during the recovery of indoor temperatures over 24 h.

The quantification of electric power consumption as a function of time serves as a valuable information for power balance. Furthermore, it is shown that during the loss of a major generation in a system with a high share of renewable power installations, active control of heating systems equipped with heat pumps provides a great flexibility, helping to prevent the frequency nadir becoming too low, causing undesirable load disconnections.

Thus, a cluster of single family houses that uses the flexibility of heating systems equipped with heat pumps has the potential to reinforce resilience in a large-scale power grid for a duration ranging from seconds to several hours.

CRediT authorship contribution statement

Sindhu Kanya Nalini Ramakrishna: Writing – review & editing, Writing – original draft, Visualization, Validation, Software, Methodology, Investigation, Formal analysis, Data curation, Conceptualization. **Torbjörn Thiringer:** Writing – review & editing, Supervision, Resources, Project administration, Conceptualization. **Peiyuan Chen:** Writing – review & editing, Supervision.

Declaration of competing interest

The authors declare that they have no known competing financial interests or personal relationships that could have appeared to influence the work reported in this paper.

Acknowledgment

The financial support provided by the Swedish Energy Agency through grant No. 50343-1 is gratefully acknowledged.

Data availability

No data was used for the research described in the article.

References

[1] Energinet, Fingrid, Statnett, Svenska kraftnät. Nordic grid development perspective 2023. 2023.

[2] Busby JW, Baker K, Bazilian MD, Gilbert AQ, Grubert E, Rai V, Rhodes JD, Shidore S, Smith CA, Webber ME. Cascading risks: Understanding the 2021 winter blackout in Texas. Energy Res Soc Sci 2021;77:102106. http://dx.doi.org/10.1016/j.erss.2021.102106.

[3] Swedish Energy Agency. Energy in Sweden 2021, an overview. 2023, [Accessed 13 July 2023].

[4] statista. Final electricity consumption in households in Sweden from 2013 to 2021, by type. 2023, [Accessed 13 July 2023].

[5] Walfridson T, Lindahl M, Ericsson N, Bergentz T, Willis M, Gustafsson O, Haglund Stignor C. Large scale demand response of heat pumps to support the national power system. In: 14th IEA, heat pump conference. 2023.

[6] Nalini Ramakrishna SK, Björner Brauer H, Thiringer T, Håkansson M. Social and technical potential of single family houses in increasing the resilience of the power grid during severe disturbances. Energy Convers Manage 2024;321:119077. http://dx.doi.org/10.1016/j.enconman.2024.119077, URL https://www.sciencedirect.com/science/article/pii/S0196890424010185.

[7] Hurtado L, Rhodes J, Nguyen P, Kamphuis I, Webber M. Quantifying demand flexibility based on structural thermal storage and comfort management of non-residential buildings: A comparison between hot and cold climate zones. Appl Energy 2017;195:1047–54. http://dx.doi.org/10.1016/j.apenergy.2017.03.004.

[8] Papaefthymiou G, Hasche B, Nabe C. Potential of heat pumps for demand side management and wind power integration in the German electricity market. IEEE Trans Sustain Energy 2012;3(4):636–42. http://dx.doi.org/10.1109/TSTE.2012.2202132.

[9] Zhang L, Good N, Mancarella P. Building-to-grid flexibility: Modelling and assessment metrics for residential demand response from heat pump aggregations. Appl Energy 2019;233–234:709–23. http://dx.doi.org/10.1016/j.apenergy.2018.10.058.

[10] Hong J, Kelly NJ, Richardson I, Thomson M. Assessing heat pumps as flexible load. Proc Inst Mech Eng Part A: J Power Energy 2013;227(1):30–42. http://dx.doi.org/10.1177/0957650912454830.

[11] Vrettos E, Andersson G. Scheduling and provision of secondary frequency reserves by aggregations of commercial buildings. IEEE Trans Sustain Energy 2016;7(2):850–64. http://dx.doi.org/10.1109/TSTE.2015.2497407.

[12] Rasmussen TBH, Wu Q, Møller JG, Zhang M. MPC coordinated primary frequency support of small- and large-scale heat pumps. IEEE Trans Smart Grid 2022;13(3):2000–10. http://dx.doi.org/10.1109/TSG.2022.3148601.

[13] Gong H, Rooney T, Akeyo OM, Branecky BT, Ionel DM. Equivalent electric and heat-pump water heater models for aggregated community-level demand response virtual power plant controls. IEEE Access 2021;9:141233–44. http://dx.doi.org/10.1109/ACCESS.2021.3119581.

[14] Muhssin MT, Cipcigan LM, Jenkins N, Slater S, Cheng M, Obaid ZA. Dynamic frequency response from controlled domestic heat pumps. IEEE Trans Power Syst 2018;33(5):4948–57. http://dx.doi.org/10.1109/TPWRS.2017.2789205.

[15] Gasser J, Cai H, Karagiannopoulos S, Heer P, Hug G. Predictive energy management of residential buildings while self-reporting flexibility envelope. Appl Energy 2021;288:116653. http://dx.doi.org/10.1016/j.apenergy.2021.116653.

[16] Papadaskalopoulos D, Strbac G, Mancarella P, Aunedi M, Stanojevic V. Decentralized participation of flexible demand in electricity markets—Part II: Application with electric vehicles and heat pump systems. IEEE Trans Power Syst 2013;28(4):3667–74. http://dx.doi.org/10.1109/TPWRS.2013.2245687.

[17] Diaz de Cerio Mendaza I, Szczesny IG, Pillai JR, Bak-Jensen B. Demand response control in low voltage grids for technical and commercial aggregation services. IEEE Trans Smart Grid 2016;7(6):2771–80. http://dx.doi.org/10.1109/TSG.2015.2465837.

[18] Baeten B, Rogiers F, Helsen L. Reduction of heat pump induced peak electricity use and required generation capacity through thermal energy storage and demand response. Appl Energy 2017;195:184–95. http://dx.doi.org/10.1016/j.apenergy.2017.03.055.

[19] Vivian J, Prataviera E, Cunsolo F, Pau M. Demand side management of a pool of air source heat pumps for space heating and domestic hot water production in a residential district. Energy Convers Manage 2020;225:113457. http://dx.doi.org/10.1016/j.enconman.2020.113457.

[20] Fischer D, Wolf T, Wapler J, Hollinger R, Madani H. Model-based flexibility assessment of a residential heat pump pool. Energy 2017;118:853–64. http://dx.doi.org/10.1016/j.energy.2016.10.111.

[21] Mendieta W, Cañizares CA. Primary frequency control in isolated microgrids using thermostatically controllable loads. IEEE Trans Smart Grid 2021;12(1):93–105. http://dx.doi.org/10.1109/TSG.2020.3012549.

[22] Péan T, Costa-Castelló R, Fuentes E, Salom J. Experimental testing of variable speed heat pump control strategies for enhancing energy flexibility in buildings. IEEE Access 2019;7:37071–87. http://dx.doi.org/10.1109/ACCESS.2019.2903084.

[23] Li X, Sun Y, Wang W, Wei W. Enhancing demand response and heating performance of air source heat pump through optimal water temperature scheduling: Method and application. Energy Build 2024;323:114839. http://dx.doi.org/10.1016/j.enbuild.2024.114839, URL https://www.sciencedirect.com/science/article/pii/S0378778824009551.

[24] Kim Y-J, Fuentes E, Norford LK. Experimental study of grid frequency regulation ancillary service of a variable speed heat pump. IEEE Trans Power Syst 2016;31(4):3090–9. http://dx.doi.org/10.1109/TPWRS.2015.2472497.

[25] Kim Y-J, Norford LK, Kirtley JL. Modeling and analysis of a variable speed heat pump for frequency regulation through direct load control. IEEE Trans Power Syst 2015;30(1):397–408. http://dx.doi.org/10.1109/TPWRS.2014.2319310.

[26] Wilczynski EJ, Chambers J, Patel MK, Worrell E, Pezzutto S. Assessment of the thermal energy flexibility of residential buildings with heat pumps under various electric tariff designs. Energy Build 2023;294:113257. http://dx.doi.org/10.1016/j.enbuild.2023.113257, URL https://www.sciencedirect.com/science/article/pii/S0378778823004875.

[27] Sperber E, Frey U, Bertsch V. Reduced-order models for assessing demand response with heat pumps – insights from the German energy system. Energy Build 2020;223:110144. http://dx.doi.org/10.1016/j.enbuild.2020.110144, URL https://www.sciencedirect.com/science/article/pii/S037877881933378X.

[28] Copeland TM. Emerson climate technologies. In: *copeland*^{TM} scroll variable speed compressors for residential air conditioning applications. Emerson Electric Co.; 2020, [Accessed 04 March 2022].

[29] Copeland Scroll. Emerson climate technologies. In: Application guidelines, scroll compressors with vapour injection for dedicated heat pumps. Emerson Electric Co.; 2004, [Accessed 04 March 2022].

[30] Nalini Ramakrishna SK, Thiringer T. Modelling of heat pumps, controller for space and water heating. Technical report, Chalmers university of technology, Gothenburg, 2024; 2024.

[31] Nalini Ramakrishna SK, Thiringer T, Markusson C. Quantification of electrical load flexibility offered by an air to water heat pump equipped single-family residential building in Sweden. In: 14^{th} IEA, heat pump conference. 2023, http://dx.doi.org/10.23697/bp31-dm12.

[32] Build Test Solutions. Ventilation and infiltration. 2025, URL https://www.buildtestsolutions.com/sectors/ventilation-and-infiltration. [Accessed 06 September 2025].

[33] Nalini Ramakrishna SK, Thiringer T. Domestic hot water heat pump: Modelling, analysis and flexibility assessment. In: 2023 IEEE PES 15th Asia-Pacific power and energy engineering conference. 2023, p. 1–5. http://dx.doi.org/10.1109/APPEEC57400.2023.10562015.

[34] Haglund Stignor C, Walfridson T. Nordsyn study on air-to-water heat pumps in humid nordic climate. In: Nordic council of ministers. 2019, http://dx.doi.org/10.6027/TN2019-502.

[35] Emerson climate technologies. Copeland scroll heating, heat pump optimized scroll technology. 2023, [Accessed 20 December 2023].

[36] Boverket. Energi i bebyggelsen – tekniska egenskaper och beräkningar– resultat från projektet BETSI.

[37] SCB statistics Sweden. Households by housing type and region, 31 December 2021. 2023, [Accessed 20 December 2023].

[38] Statistics Sweden, SCB. Just over 4.9 million dwellings in Sweden. 2023, [Accessed 20 December 2023].

[39] Blom N. Folkhälsomyndighetens allmänna råd om temperatur inomhus. Folkhälsomyndigheten; 2014.

[40] Hedbrant J. On the thermal inertia and time constant of single-family houses. In: Licentiate dissertation, linköpings universitet, linköping. 2001.

[41] Alvarez MAZ, Agbossou K, Cardenas A, Kelouwani S, Boulon L. Demand response strategy applied to residential electric water heaters using dynamic programming and K-means clustering. IEEE Trans Sustain Energy 2020;11(1):524–33. http://dx.doi.org/10.1109/TSTE.2019.2897288.

[42] Engineering ToolBox. Average overall heat transmission coefficients for fluid and surface combinations like water to air, water to water, air to air, steam to water and more. 2022, URL https://www.engineeringtoolbox.com/overall-heat-transfer-coefficients-d_284.html. [Accessed 31 June 2022].

[43] Lundh M, Wäckelgård E, Ellegård K. Design of hot water user profiles for Swedish conditions. In: Goswami DY, Zhao Y, editors. Proceedings of ISES world congress 2007 (vol. i – vol. v). Berlin, Heidelberg: Springer Berlin Heidelberg; 2009, p. 2074–8.

[44] Statistics Sweden, SCB. Most children live in one- or two-dwelling buildings. 2023, [Accessed 20 December 2023].

[45] IEEE, Power System Dynamic Performance Committee. Test systems for voltage stability analysis and security assessment. 2023, PSS/E model, [Accessed 14 August 2023].

[46] Van Cutsem T, Glavic M, Rosehart W, Canizares C, Kanatas M, Lima L, Milano F, Papangelis L, Ramos RA, Santos JAd, Tamimi B, Taranto G, Vournas C. Test systems for voltage stability studies. IEEE Trans Power Syst 2020;35(5):4078–87. http://dx.doi.org/10.1109/TPWRS.2020.2976834.

[47] Saarinen L. A hydropower perspective on flexibility demand and grid frequency control. In: Uppsala universitet, Uppsala. 2001.

[48] Pourbeik P. Proposal for new features for the renewable energy system generic models. 2023, URL https://www.wecc.org/Administrative/Memo_RES_Modeling_Updates_010523_Rev25_Clean.pdf.

[49] Ullah NR, Thiringer T, Karlsson D. Temporary primary frequency control support by variable speed wind turbines— potential and applications. IEEE Trans Power Syst 2008;23(2):601–12. http://dx.doi.org/10.1109/TPWRS.2008.920076.

[50] Imgart P, Beza M, Bongiorno M, Svensson JR. An overview of grid-connection requirements for converters and their impact on grid-forming control. In: 2022 24th European conference on power electronics and applications. 2022, p. 1–10.

[51] Herre L, Nourozi B, Hesamzadeh MR, Wang Q, Söder L. Provision of multiple services with controllable loads as multi-area thermal energy storage. J Energy Storage 2023;63:107062. http://dx.doi.org/10.1016/j.est.2023.107062, URL https://www.sciencedirect.com/science/article/pii/S2352152X23004590.

[52] Svenska kraftnät. Overview of the requirements for reserves. Svenska kraftnät; 2022.

[53] Wang X, Gao W, Scholbrock A, Muljadi E, Gevorgian V, Wang J, Yan W, Zhang H. Evaluation of different inertial control methods for variable-speed wind turbines simulated by fatigue, aerodynamic, structures and turbulence (FAST). IET Renew Power Gener 2017;11(12):1534–44. http://dx.doi.org/10.1049/iet-rpg.2017.0123, URL https://ietresearch.onlinelibrary.wiley.com/doi/abs/10.1049/iet-rpg.2017.0123.

[54] El Itani S, Annakkage UD, Joos G. Short-term frequency support utilizing inertial response of DFIG wind turbines. In: 2011 IEEE power and energy society general meeting. 2011, p. 1–8. http://dx.doi.org/10.1109/PES.2011.6038914.